Design and Fabrication of a Novel Hybrid Solar Dryer

Cheruka Perera[1], Gayashika Fernando[2] , Migara Liyanage[2]
[1]School of Civil and Mechanical Engineering, Faculty of Science and Engineering, Curtin University, Kent St, Bentley WA 6102, Australia
[2] Faculty of Engineering, Sri Lanka Institute of Information Technology
New Kandy Rd, Malabe, 10115, Sri Lanka

gayashika.f@sliit.lk , migara.l@sliit.lk
Corresponding author: c.devanaguruge@graduate.curtin.edu.au

ABSTRACT

A hybrid solar dryer was designed and tested for commercial dissemination of active and passive drying methods over traditional sun drying methods. The proposed dryer employs novel features such as user controllability of the drying parameters and includes sensors and controllers for active monitoring of drying parameters. The functionality of the dryer is broadened by using logic control whereby intermittent drying patterns are introduced to the system for more efficient operation. This paper documents the design calculations and fabrication process of the dryer as well as the results of drying obtained under a controlled environment.

10 experiments have been carried out to assess the limits and potential improvements to the system which yielded satisfactory conditions with a temperature fluctuation of ± 1℃ and change in %RH of $\pm 2\%$ at any given temperature within the specified limits. The developed system has been used for drying apples which yielded dried products from an initial weight of 346 grams to a final weight of 55 grams in 5 hours in pure convection and the same initial weight was reduced to 52 grams in 3 hours when operating in solar hybrid mode. The average energy consumption of the dryer was obtained at 300 Watts at uninterrupted solar insolation operation and 224 Watts during pure convective operation, portraying the efficient operation of the system to be eligible to be powered by a solar-powered energy storage

KEYWORDS: *Solar-Hybrid Drying, Convective Drying, Design, Fabrication.*

1 INTRODUCTION

Drying is a method of preserving hygroscopic foods for prolonged periods by dehydration. The drying process is an energy-intensive process accounting for 15-20% of energy consumption in the food industry. And when commercial drying systems decline in efficiency, the mentioned usage percentage can reach as high as 30-33%. Due to the declining availability of non-renewable energies, there has been a major requirement to find alternative energies to drive this process. Solar energy is the most abundant energy source that is also the most easily obtainable source of energy to fulfill the energy requirement.

The main disadvantage however is the inconsistency of supply, mainly during nighttime. Due to this reason, traditional greenhouse dryers are not self-sustained for long operating periods. Hence the requirement arises to implement an alternative energy source for the dryer to be operable regardless of solar irregularities and time of day. This paper proposes a novel hybrid solar dryer that utilizes direct solar irradiation and electrical energy stored through a photovoltaic panel to be utilized in the process of drying and be robust to climatic changes.

Hybrid dryers that utilize two or more energy sources have existed since past times. Designs have originated from passive dryers which use the greenhouse effect to increase the temperature inside the drying chamber, and buoyant flow for evacuating humid air volumes outside the drying chamber. (Sharma et al., 1986) designed their natural convection dryer for rural areas which consisted of solar-powered drying, and buoyance-assisted flow (natural flow). They started by laying the mathematical foundation required for the parametric design of the dryer and fabrication. They have concluded their

ISSN 2961-5011 | https://doi.org/10.54389/CLYB6448

results stating that a span of 3 days was required to dry 10kg of green peas (Estimated energy requirement – 18.4MJ). The passive drying technique evolved to an active drying technique where forced draft is used to evacuate humid volumes outside of the system without depending on the buoyant flow. Authors who attempted to compare the three techniques have yielded exponentially improved results when using active drying. (Pochont et al., 2020) have carried out a comparative study in drying red chilli by methods of greenhouse drying (Active and Passive mode) and open sun drying. They have achieved a reduced time of drying by 50% in passive drying and 54.1% in active drying. They also reached a lower moisture content in active mode (18.67% wet basis) and passive mode (18.7%) compared to open sun drying method (24.24%). By view of this, it is observed that the process is capable of being hybrid powered especially being a country closer to the equator the annual GHI of Sri Lanka is evaluated at $2000 kWh/m^2$.

When implementing an efficient system for drying it is important to understand the drying kinetics. Understanding the kinetics allows an individual to identify times at which the drying rate can be increased by increasing temperature, without causing damage to the products and times which the system can run at a low energy intensive mode while yielding the same results as continuous drying. Drying of hygroscopic material is divided into two main phases of operation based on the surface moisture content and the product properties at a cellular scale, such as diffusivity, thermal conductivity etc.

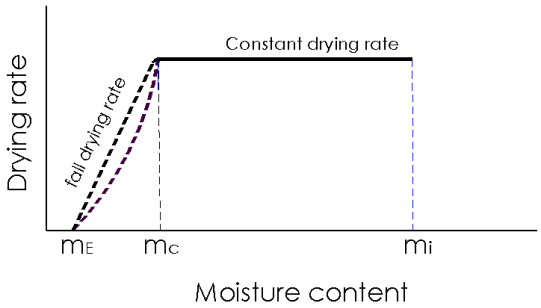

Figure 1 Phases of drying

The drying rate of a hygroscopic product usually adheres to this behavior which is confirmed by numerous studies relating to this area. Initially, the constant rate drying period where the product contains surface moisture which allows free evaporation. At this stage, the drying rate is governed by the properties of the inflow (Temperature, Humidity, etc.), where the temperature can be increased to achieve high drying rates while the products are stabilized at the wet-bulb temperature. Once this free moisture layer is depleted, further drying requires the product to transport internal moisture to the surface of the product which is governed by the thermal and physical characteristics (Moisture diffusivity and thermal conductivity) of the cellular structure. At this stage of drying, internal heating of the product is crucial to maintain moisture transportation from within the product. Simply increasing the drying temperature as previously, would result in case hardening of the products (Gulati and Datta 2015). As per studies investigated, solar irradiation is an excellent source for providing the required internal heating compared to convective heat transfer which can only heat the products to drying temperature. Hence, theoretically by using direct solar irradiation, the process should be faster compared to pure convective drying.

Most designs incorporate manual control of the flow and temperature but do not possess the feature to control humidity. As explained in the drying curves, it is beneficial to adjust the drying conditions at different stages of drying to obtain several major advantages. The process of actively adjusting the conditions is defined as ‘intermittency’. Several authors have investigated the effect of intermittent drying on various products (Foods, Clay, Ceramic), where they have made a common conclusion that intermittent drying not only expedites the process but also majorly reduces the energy demand (Kowalski and Pawłowski 2011; Kumar, Karim, and Joardder 2014; da Silva et al. 2015).

This research aims to develop a solar hybrid dryer capable of continuous operation, robust to the changes in climatic conditions, incorporating renewable energy sources for driving the drying process. The novel design offers features such as temperature, airflow, and humidity control. The suggested design incorporates a microcontroller operating as the brains of the system. This allows active control of the parameters of drying, either to be set as a constant value or a variable value dictated by the algorithm. This yields advantages such as the autonomous operation of the dryer without human interaction, robustness to changing weather conditions, and intermittent patterns of drying to adjust the quality of the output product (da Silva et al. 2015).

2 DESIGN AND FABRICATION

2.1 Dryer design

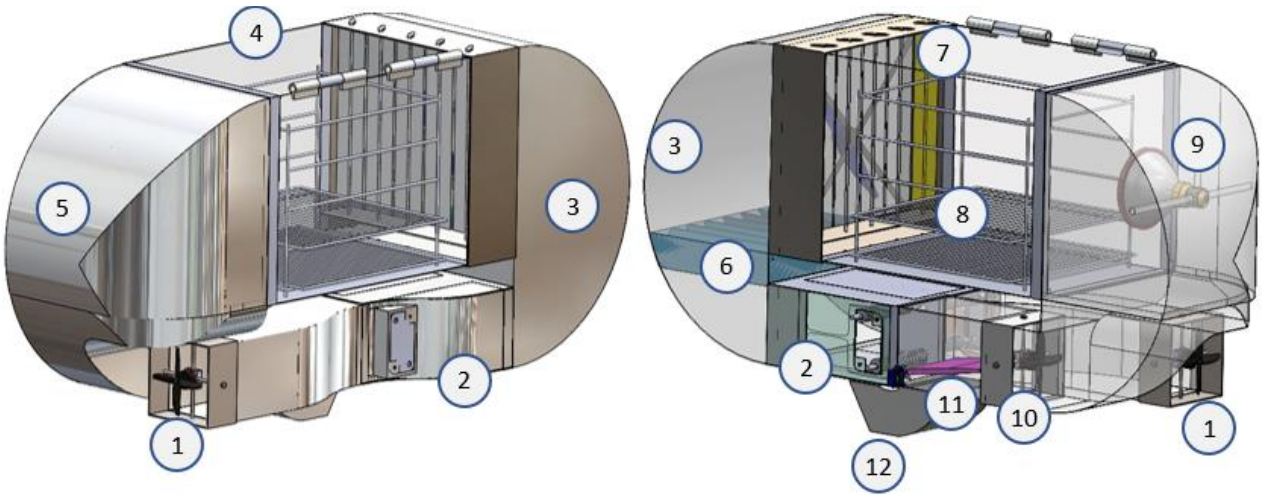

Figure 2 Dryer design (Visual representation - Left, Internal representation – Right)

Table 1. Description

Index	Description
1	Ambient air intake (tertiary propeller)
2	Heating port
3	Circulation duct
4	Drying chamber
5	Funnel duct
6	Mixer vent
7	Infrared screens and the primary propeller
8	Drying Shelves
9	Infrared source (Conceptual)
10	Secondary propeller
11	Recycling gate
12	Exhaust

The design is mainly focused on minimizing the thermal and aerodynamic losses of the system. The unusual shape of the system originates from the tangent curves of the ducts which provide the smooth translation of the flow vector by 180 degrees. The combination of two ducts provides the full 360 degrees of circulation of the drying air which allows to partially recycle the flow back into the system for preserving thermal energy. In addition to recirculation, external surfaces exposed to ambient conditions have also been insulated using thermal foil to further improve the thermal efficiency of the system.

Many solar dryer designs incorporate a flatbed drying surface (>1 m in width) for high solar absorption (Amer, Hossain, and Gottschalk 2010; Pochont et al. 2020a), but the new design is expected to operate at night time, hence to reduce the adverse heat loss to the ambient at nighttime, the drying chamber is designed to be narrow which allows sufficient insolation into the drying chamber (0.3 m). Compared to designs that incorporate induced draft (Laminar flow) in the drying chamber (Reyes et al. 2013), the new design uses forced draft to generate turbulent airflow which aids in heat and mass transfer from the products.

When the dry air passes the drying chamber, it gathers moisture and proceeds to the funnel duct. The funnel shape along with the secondary propeller directs the air into the recycling gate. A humidity probe placed before the gate detects the humidity of the exhaust flow and opens the gate at a precise angle to facilitate partial exhaust of drying air. This helps to maintain a set humidity in the drying chamber by equating the vapor extracted from the drying chamber to vapor exhausted at the gate. Similarly, Temperature control is achieved by sensors placed in the path of flow which triggers the activation of the heater coils based on the value read by the sensors (A tolerance is introduced to bypass sensor errors). Through autonomy, the heating system can operate for pulses of variable widths dictated by the standard logic algorithms that control the system.

The design constitutes 3 propellers of different sizing to facilitate airflow across the system at required flow rates. A 10-inch propeller is used in the drying chamber to match the $11.8 \times 11.8\ in^2$ cross section of the chamber. The propeller initiates turbulent rectilinear flow within the drying chamber, which aids efficient heat transfer to the products and vapor mass transfer from the products. Similarly, the secondary propeller and tertiary propellers are sized to match the cross section of the respective ducts to achieve rectilinear flow. The speed of the brushless motors is adjusted through 3 phase speed controllers using a PMW signal generated by the microcontroller.

The heating of the flow is achieved through coiled Nichrome wires of 20 AWG installed in the heating duct. The power required for heating is supplied through a custom 50 VAC transformer capable of providing 15 Amps at 45 VAC, which leads to $\approx 650\ Watts$ of power dissipation at the heater coils. Asbestos and Mica have been used selectively for electrical resistance and high heat application of the heating duct. Current flow to the heater coils is controlled through a bta41600b Triac (40 A capacity) and an optocoupler arrangement. This allows for the current to be easily controlled by adjusting the 'gate' current of the transistor. The optocoupler isolates the microcontroller from the high voltage paths which ensures component safety.

It should be noted that the system was originally designed to operate at 12 V DC since high current sources (12 V) were readily available in the market for low prices. However, to produce high heat (2.3 KW) at 12 V would require a nichrome wire of 4.8 mm Diameter (5 AWG), which is not commercially available. Additionally, the lowest gauge of wire available at the time of fabrication was 20 AWG which required moderately high voltage to produce ample heat as calculated above.

2.2 Fabrication

Fabrication of the flow ducts has been mainly done by using Galvanized aluminum sheets of 0.5mm gauge. The selected gauge is easily formable and can be fabricated to required shapes using common household tools. Additionally, the galvanized property prevents corrosion under high humidity and temperatures. Once the 3D model was constructed, the surfaces were converted into 2D geometries using the CAD software ('SOLIDWORKS') and individual surfaces were fabricated using the sheet metal and joined together using rivets, epoxies, and silicone. Galvanized iron sheets of 1mm gauge were used to construct the skeleton structure for holding the individually fabricated ducts in place. Gauge was selected based on the weight of the structure to ensure no deformation in the structure would occur. The deformation could lead to moving parts (Propellers, Gates) colliding with the enclosed surfaces.

Material selection of the system based on prior assessment of the application has led to the inexpensive and fast fabrication of the system. Additionally, utilizing the CAD model to aid the fabrication process has led to the precise fabrication of the parts which were joined together to obtain the rigid structure without the need for any fasteners (Fasteners were used for additional safety). Direct insolation provisions in the drying chamber are provided using Polycarbonate sheets of 3mm gauge and silicone is used for airtight sealing of air ducts and the drying chamber.

Drying shelves are constructed using steel rods of 2mm spaced by 20mm to facilitate uninterrupted radiation to the bottom shelves and maintain airflow through the chamber.

Figure 3 Fully fabricated system

2.3 Cost

The build of the system for operation based on grid electricity requires an estimated cost of 75 000 LKR. The cost has been heavily impacted by the recent increase in the price of material and other equipment. Based on experiments, when the system is running at its highest settings ($50℃, 20\%RH, Hybrid\ mode$), the average power consumption was valued at $\approx 300W$. Whereas, when solar power is unavailable, the system could operate at a temperature of $45℃$ with an average power consumption of $\approx 230\ W$. Based on the following data, for 24 hour operation of the system, an electrical storage of 300 Ah and a Solar panel with a rated output of $\approx 700\ Watts$ along with the charge controlling equipment would be required to power the system at its standard operating conditions ($45℃$).

It should be noted that the required components (Nichrome wire of required gauge, Thermocouples, Heat insulation etc.) could not be obtained at the time of fabrication due to unavailability of stock. Hence 40% of the cost (30000LKR) has been spent on implementing a 50 VAC transformer to power the nichrome wires of 22 AWG, to produce the heating requirement of $650\ Watts$. The cost would reduce to 50000 LKR if a lower gauge nichrome wire coupled with a high current source at 12 V could be used.

2.4 Controlling parameters

- Temperature control

As mentioned previously, temperature control of the system is achieved through a sensor and feedback system which activates the heater coil circuitry as required.

$$(\dot{Q}_{Loss} + \dot{Q}_{Drying})t_{cycle} = mC_p\Delta T_{air} = \dot{Q}_{Heater} \times t_{active} \quad (1)$$

Where,

$\dot{Q}_{Loss} + \dot{Q}_{Drying}$	Heat requirement for isothermal operation
t_{cycle}	Cycle time at standard circulation speed
m	Mass of air
C_p	Specific energy of air at constant pressure
ΔT_{air}	Temperature change per cycle
$\dot{Q}_{Heater}$	Heat input to the system/ Heat output from heater coils
t_{active}	Time of activation

Temperature is continuously decreased due to heat loss and heat absorbed by the products. Temperature is maintained by assessing this heat loss by terms of temperature difference (ΔT_{air}) in subsequent cycles of circulation, the required duration of activation (t_{active}) can be calculated from the equation above where the coil output can be calculated by measuring the current and the voltage of the source ($\dot{Q}_{Heater} = VI$).

- Humidity control

Humidity control is achieved through the following governing equation of vapor balance

$$\omega_{Drying} = R\left(\omega_{Initial} + \frac{\dot{m}_{Vapor}}{\dot{m}_{Air}}\right) + (1 - R)\omega_{atmos} \quad (2)$$

ω_{Drying}	Absolute humidity in drying chamber (User specified)
R	Recycling rate (Algorithm dictated)
$\omega_{Initial}$	Absolute humidity after absorbing vapor from the chamber
$\dot{m}_{Vapor}$	Rate of vapor extraction
$\dot{m}_{Air}$	Rate of airflow from the ambient
ω_{atmos}	Atmospheric absolute humidity

The chamber absolute humidity 'ω_{Drying}' is a function of the Recycling rate 'R' used at the recycling gate. 'ω_{Drying}' can be controlled regardless of the rate of vapor absorption in the chamber '$\dot{m}_{Vapor}$' by controlling the value of 'R' but would require high energy input as heat recovery from the exhaust will be low at low recycling rates.

Absolute humidity is considered in calculations which indicates the mass of water vapor in the atmosphere, independent of the temperature. Since the drying chamber and the atmosphere function at different temperatures, absolute humidity provides common grounds for performing humidity calculations and reference to psychrometry.

Experiments have been conducted to assess the stability of the humidity and temperature of the system explained through the equations in the previous section. The parameters are controlled by a standard logic code (C++) that reads sensor feedback and compares it with the user specified values of temperature and humidity and performs actions accordingly. During experimentation, Temperature stability has been obtained at the set value, oscillating between the high and low bounds set by the algorithm. Stability of humidity has also been achieved in the drying chamber at a satisfactory deviation of $\pm 2\%\ RH$.

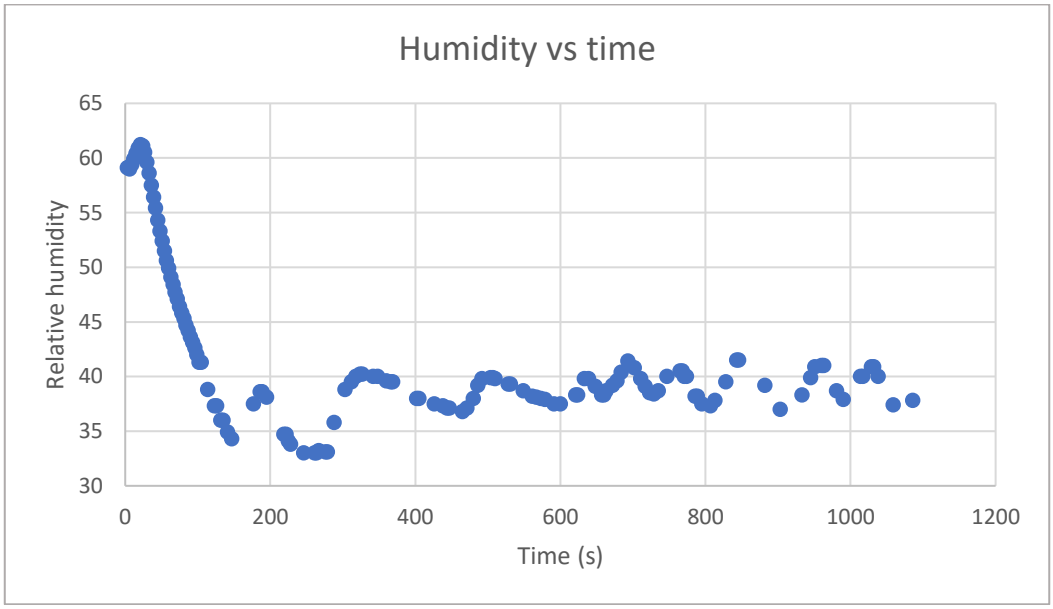

Figure 4 Humidity behavior when stabilized at 40%RH

3 EXPERIMENTS AND RESULTS

Experiments were conducted based on the two operating modes of the dryer. Pure convective mode which utilizes generated heat at the coils to drive the process, and Hybrid mode which utilizes both generated and solar heat to drive the process. Following steps have been followed in both experiments to establish uniformity of the process.

Methodology:

- Fresh green apples at ambient conditions have been sliced to $\approx 3mm$ thick slices and obtained at 346 g of mass.
- Slices are evenly distributed on the 5 trays for drying and dried at conditions of $45℃$ in pure convective drying and $50℃$ in hybrid mode.
- Subjects are taken out of the chamber at equal periods of elapsed time (30 minutes) and measured using a scale of $\pm\ 1g$ accuracy
- The weight reading is recorded with the respective time of measurement
- The procedure is carried out until a weight reduction of $\Delta W \leq \pm\ 2g$ was achieved.

3.1 Sequential experiments

Pure convective mode

Table 2 Control parameters for convective drying

Chamber Temperature	45 ± 1 ℃ (max $capacity$)
Chamber humidity	$40 \pm 3\%$ RH
Flow velocity	$1.2\ ms^{-1}$

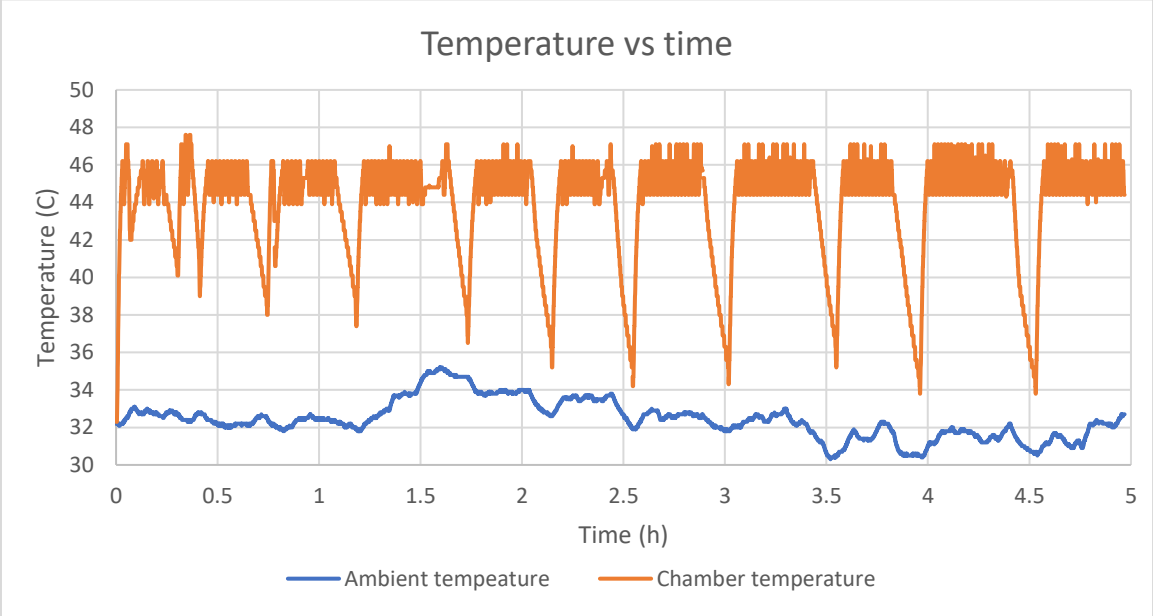

Figure 5 Temperature vs time behavior of convective drying

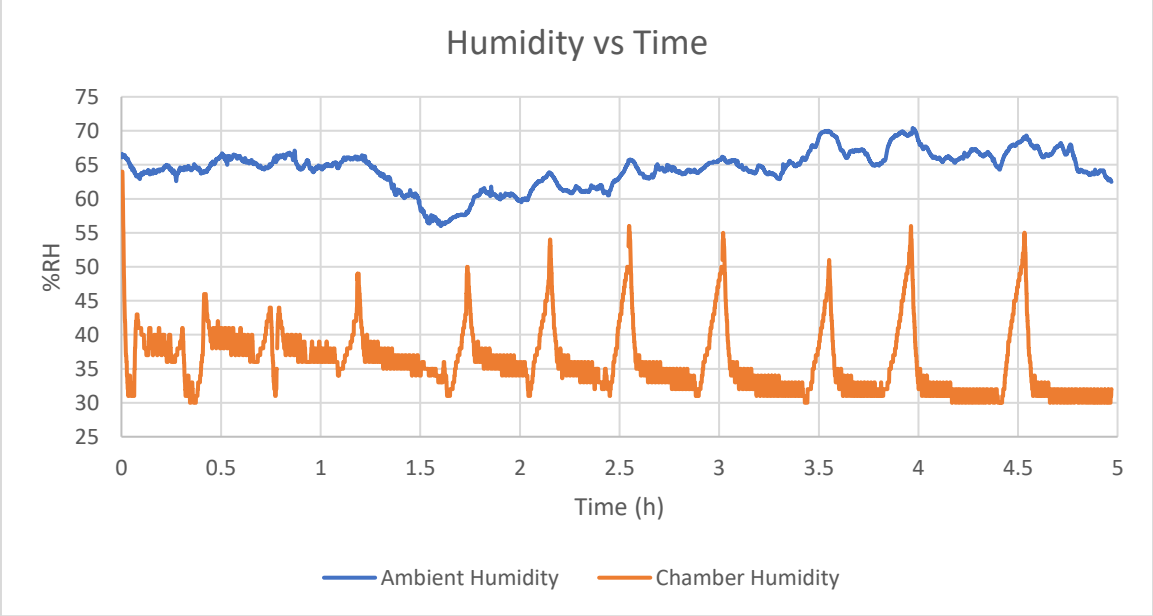

Figure 6 Humidity vs time behavior of Convective drying

- The spikes in the charts correspond to the unloading and loading of the subjects when obtaining weight readings.

Hybrid mode

Table 3 Control parameters for Hybrid drying

Chamber Temperature	50 ± 1 ℃ (max $capacity$)
Chamber humidity	$20 \pm 3\%$ RH
Flow velocity	$1.2\ ms^{-1}$

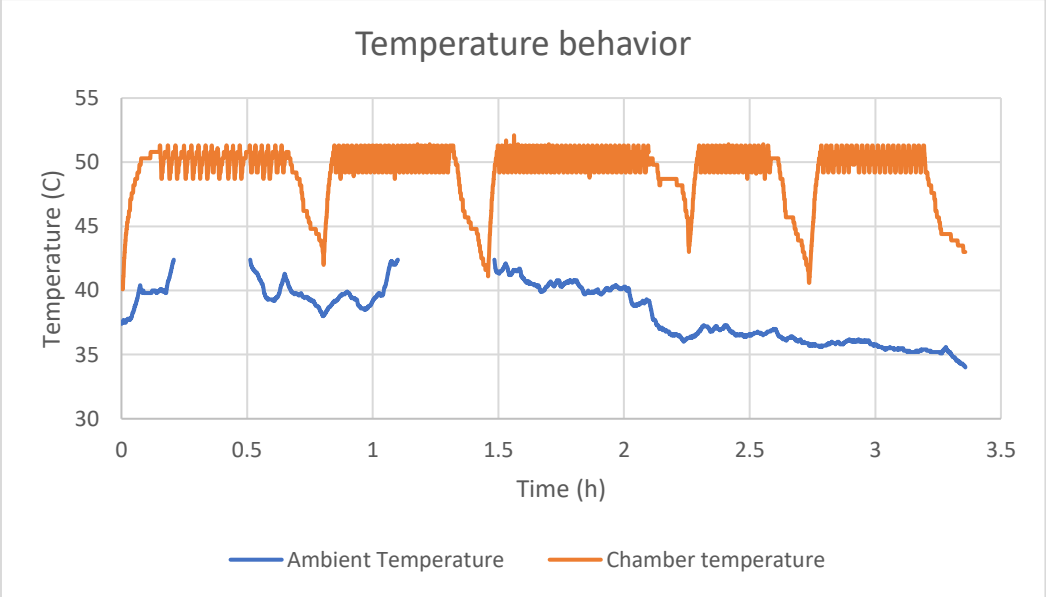

Figure 7 Temperature vs time behavior of hybrid drying

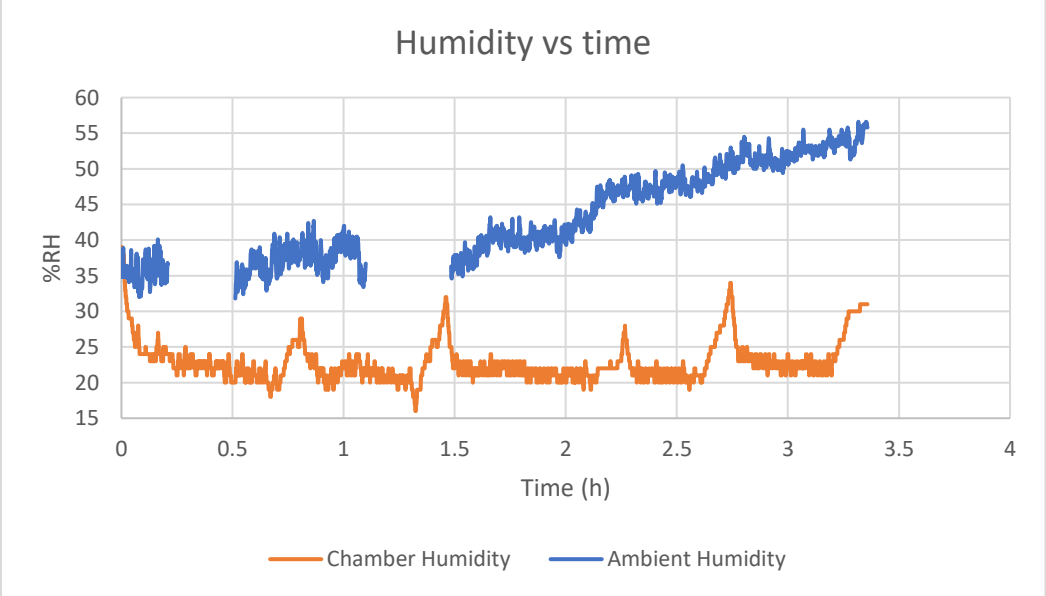

Figure 8 Humidity vs time behavior of hybrid drying

The main disadvantage of designs proposed by previous designs is the dependency of drying conditions on atmospheric conditions. Although the temperature is well controlled by using various techniques, most designs do not propose a method for humidity control. By the figures represented above, it can be acknowledged that the system is robust to changes in the atmospheric temperature and humidity, by using the microcontroller to process the feedback from the sensors and manage the properties accordingly (Section 2.4).

3.2 Results comparison

Figure 9 Visual comparison of the subjects dried under different modes (Before drying, Convective drying and solar hybrid drying)

By visual comparison of the subjects, it can be observed that the convective drying process has led to more browning of the subjects. Sundried samples at 50 C temperature seemed to be visually more appealing compared to convective drying at 45 C. At low temperatures, moisture remains for a longer duration on the surface which spans the chemical process of browning for a longer time, whereas at 50 C, the moisture is rapidly removed from the surface stalling the process of browning. As mentioned in section 1, high drying rates cause the moisture routes to shrink and impair the product of being further dried, hence the samples dried at 50 C further reduce the browning effect by trapping the moisture within the product.

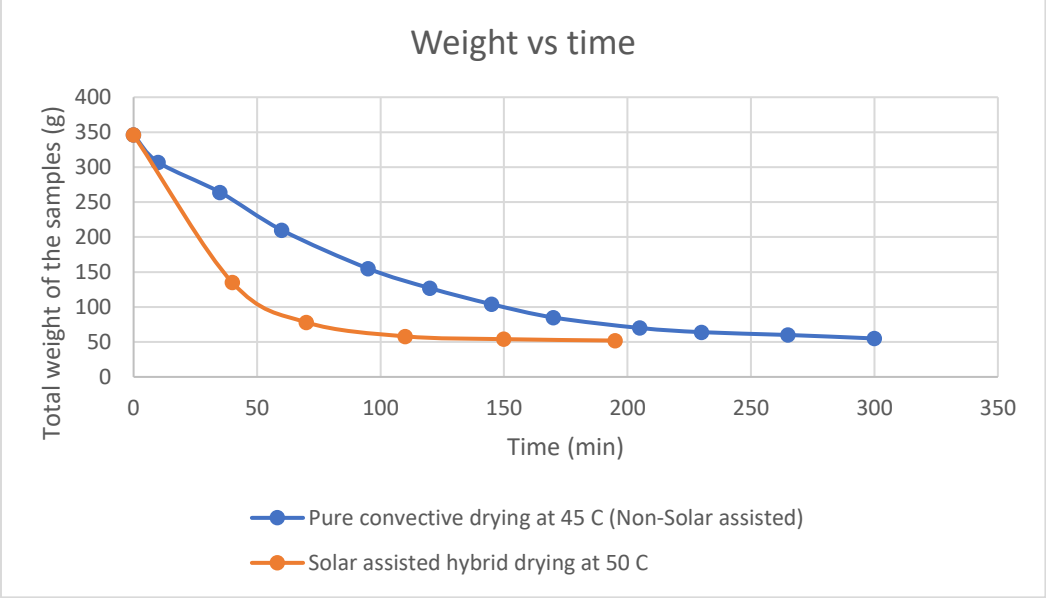

Figure 10 Rate of weight reduction in two modes of drying

It can be observed that the convective mode at 45 ℃ concluded the drying process (from 346g initial weight to 55g final) in 300 minutes whereas the hybrid mode performed the process (from 346g initial weight to 52g final) in 195 minutes. This experiment indicates substantial improvement in drying time when using high temperatures assisted by solar radiation. Hence, it can be stated that a solar incorporated hybrid dryer would enhance the performance of the system when drying is performed at intermediate temperatures (45<T<60) (Jeevarathinam et al. 2021). As mentioned in section 1, the curved shape of moisture reduction is due to the conversion of the hygroscopic subject from saturated surface moisture to transporting moisture from the inner cellular structure.

Drying at this stage requires high internal heating of the product, which can be supplied by increasing the convective temperature to $60 - 70℃$ or exposure to high intensity infrared waves/ Solar insolation. The convective temperature is limited by the heat output at the coils and solar insolation cannot be controlled, hence an infrared source is proposed (Section 2.1) to increase the functionality of the system.

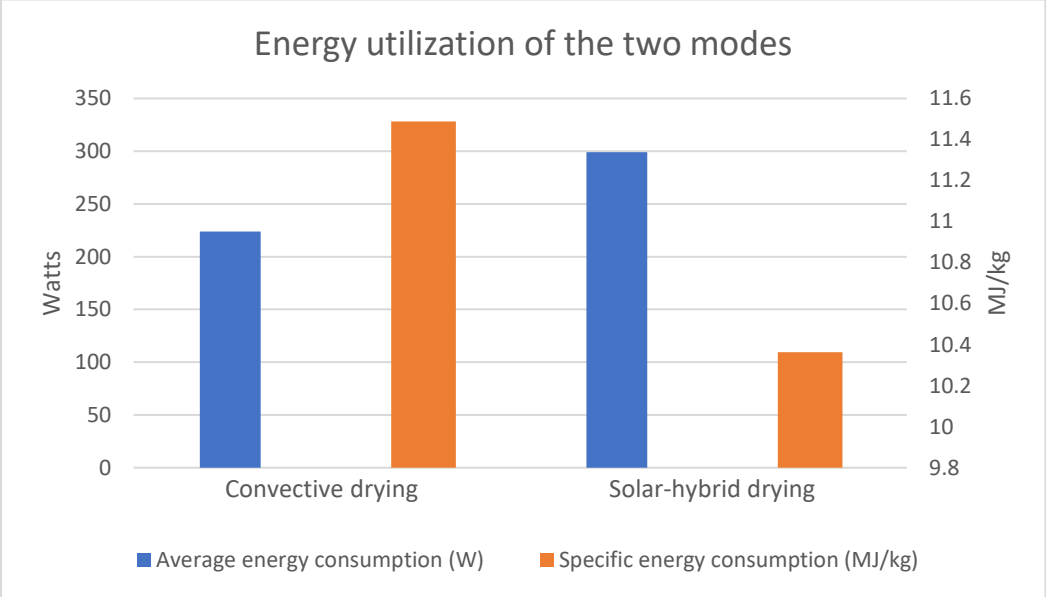

Figure 11 Energy utilization when drying from two methods

Studies of (EL-Mesery et al., 2021), have concluded the importance of direct radiation in drying apple slices as it could significantly increase the rate of heat transfer to the internal body of the product compared to convective heat transfer. As observed in the following figure, the specific energy consumption when operating in hybrid mode resulted in a significantly less magnitude when compared to pure convective drying. Inducing high heat conduction rates to the inside of the product can aid the rapid transportation of moisture from inside of the product, thereby reducing drying times and energy requirement to dry a kilogram of the product (Specific energy). When comparing the obtained results, they have observed an SEC of 12.72 MJ/kg when drying apple slices at $30℃$ at an infrared intensity of $0.15\ Wcm^{-2}$, whereas the author conducted the experiment at $50\ ℃$ at a similar infrared intensity (Solar) and observed an SEC of 10.4 MJ/kg. SEC has been improved due to increased moisture absorption at high temperatures due to low %RH. Additionally, increasing the density of drying material in the drying chamber also helps to increase the efficiency of the dryer as the rate of heat transfer to the products is increased.

4 CONCLUSION

A solar hybrid dryer was designed and built to determine the effect of incorporating solar irradiation in the convective drying process. The dryer was able to reach higher temperatures, $50℃$ in hybrid mode compared to $45℃$ in convective mode. As a result, a 10% saving in specific energy consumption was achieved when drying in hybrid mode compared to convective mode. As previously explained, direct irradiation to the products yielded a significantly less time of processing compared to convective mode and also led to a lower moisture content (-3 g) at the end of the experiment. The average energy consumption when drying in Hybrid mode was 300W at $50℃$, which proves the eligibility of the system to be powered by photovoltaic electrical energy storage.

5 ACKNOWLEDGEMENTS

I would like to convey my sincere gratitude towards Prof. Migara Liyanage and Dr. Gayashika Fernando for their guidance, support and providing expert knowledge for the betterment of my progress. Furthermore, investing their valuable time in providing feedback and instructions to overcome the difficulties faced in the duration of the project.

REFERENCES

Amer, B. M.A., M. A. Hossain, and K. Gottschalk. 2010. "Design and Performance Evaluation of a New Hybrid Solar Dryer for Banana." *Energy Conversion and Management* 51 (4): 813–20. https://doi.org/10.1016/j.enconman.2009.11.016.

EL-Mesery, Hany S., Reham M. Kamel, and Ramy Z. Emara. 2021. "Influence of Infrared Intensity and Air Temperature on Energy Consumption and Physical Quality of Dried Apple Using Hybrid Dryer." *Case Studies in Thermal Engineering* 27 (April): 101365. https://doi.org/10.1016/j.csite.2021.101365.

Gulati, Tushar, and Ashim K. Datta. 2015. "Mechanistic Understanding of Case-Hardening and Texture Development during Drying of Food Materials." *Journal of Food Engineering* 166: 119–38. https://doi.org/10.1016/j.jfoodeng.2015.05.031.

Jeevarathinam, G., R. Pandiselvam, T. Pandiarajan, P. Preetha, M. Balakrishnan, V. Thirupathi, and Anjineyulu Kothakota. 2021. "Infrared Assisted Hot Air Dryer for Turmeric Slices:Effect on Drying Rate and Quality Parameters." *Lwt* 144 (September 2020). https://doi.org/10.1016/j.lwt.2021.111258.

Kowalski, S. J., and A. Pawłowski. 2011. "Energy Consumption and Quality Aspect by Intermittent Drying." *Chemical Engineering and Processing: Process Intensification* 50 (4): 384–90. https://doi.org/10.1016/j.cep.2011.02.012.

Kumar, Chandan, M. A. Karim, and Mohammad U.H. Joardder. 2014. "Intermittent Drying of Food Products: A Critical Review." *Journal of Food Engineering* 121 (1): 48–57. https://doi.org/10.1016/j.jfoodeng.2013.08.014.

Pochont, Nitin Ralph, Mohammad Noor Mohammad, Bodepu Thrinadh Pradeep, and P. Vijaya Kumar. 2020a. "A Comparative Study of Drying Kinetics and Quality of Indian Red Chilli in Solar Hybrid Greenhouse Drying and Open Sun Drying." *Materials Today: Proceedings* 21: 286–90. https://doi.org/10.1016/j.matpr.2019.05.433.

———. 2020b. "A Comparative Study of Drying Kinetics and Quality of Indian Red Chilli in Solar Hybrid Greenhouse Drying and Open Sun Drying." In *Materials Today: Proceedings*, 21:286–90. Elsevier Ltd. https://doi.org/10.1016/j.matpr.2019.05.433.

Reyes, Alejandro, Andrea Mahn, Francisco Cubillos, and Pedro Huenulaf. 2013. "Mushroom Dehydration in a Hybrid-Solar Dryer." *Energy Conversion and Management* 70 (June): 31–39. https://doi.org/10.1016/J.ENCONMAN.2013.01.032.

Sharma, V. K., S. Sharma, R. A. Ray, and H. P. Garg. 1986. "Design and Performance Studies of a Solar Dryer Suitable for Rural Applications." *Energy Conversion and Management* 26 (1): 111–19. https://doi.org/10.1016/0196-8904(86)90040-3.

Silva, Wilton Pereira da, Andréa Fernandes Rodrigues, Cleide Maria D.P.S. E Silva, Deise Souza de Castro, and Josivanda Palmeira Gomes. 2015. "Comparison between Continuous and Intermittent Drying of Whole Bananas Using Empirical and Diffusion Models to Describe the Processes." *Journal of Food Engineering* 166: 230–36. https://doi.org/10.1016/j.jfoodeng.2015.06.018.